Oxygenic Photosystem II: The Mutation D1−D61N in *Synechocystis* sp. PCC 6803 Retards S-State Transitions without Affecting Electron Transfer from Y_Z to P_{680}^+ †

Monika Hundelt,‡ Anna-Maria A. Hays,§ Richard J. Debus,§ and Wolfgang Junge*,‡

Abt. Biophysik, Universität Osnabrück, D-49069 Osnabrück, Germany, and Department of Biochemistry, University of California, Riverside, California 92521-0129

Received May 18, 1998; Revised Manuscript Received July 22, 1998

ABSTRACT: Photosynthetic oxygen evolution is powered by photosystem II (PSII), in particular by the oxidized chl *a*-aggregate P_{680}^+, and catalyzed by the oxygen-evolving complex (Mn_4X-entity) as well as a tyrosine residue (Y_Z). The role of particular amino acids as cofactors of electron and proton transfer or as modulators of the activity is still ill-defined. The effects of single-site mutations at the donor side of PSII on the partial reactions of water oxidation have been primarily studied in whole cells. Because of better signal-to-noise in oxygen-evolving core preparations more detailed information on the electronic, protonic, and electrostatic events is expected from studies with such material. We investigated cells and oxygen-evolving core preparations from the wildtype of *Synechocystis* sp. PCC 6803 and point-mutants of D1−D61. In cells, oxygen-release was slowed drastically in D61A (8-fold) and D61N (10-fold) compared to WT, whereas it remained unchanged in D61E within the time resolution of the measurements. In core preparations, the $S_1 \Rightarrow S_2$ and $S_2 \Rightarrow S_3$ transitions were slowed approximately 2-fold in D61N compared to WT. However, the nanosecond components of electron transfer from Y_Z to P_{680}^+ were unchanged in the same mutant. We conclude that substitution of a neutral residue for D1−D61 selectively affects electron-transfer events on the donor side of Y_Z.

1. INTRODUCTION

Photosystem II (PSII)[1] of green plants and cyanobacteria produces dioxygen from two water molecules at the expense of four quanta of light. Absorption of light induces a charge separation between a chl *a*-entity, P_{680}, and bound plastoquinone, Q_A, to yield P_{680}^+ and Q_A^-. P_{680}^+ is reduced in nanoseconds by Y_Z (Tyr-161 on the D1 subunit). Y_Z^{ox}, in turn, is reduced by the oxygen evolving complex (OEC) stepping it forward from state S_0 to S_4. S_4 spontaneously decays into S_0 under release of dioxygen.

Whether the Mn_4 complex is the only redox cofactor of the OEC or whether an amino acid cofactor (His?, Tyr?) is also involved is under contention (reviewed e.g. in refs *1*−*4*). The structure of the donor side is only evolving. Because electron crystallography with PSII is presently only at 0.8 nm resolution (*5*), the structural information is very limited and is based on modeling (e.g. refs *6* and *7*) in analogy to the bacterial reaction center (*8*), optical spectroscopy (*9*−*12*) and EPR (*13*−*17*).

Mutants from *Synechocystis* sp. PCC 6803 of the residue D1-Asp61, located in the lumenal loop between helices A and B (*18*), have been studied with cells (*19*). In the latter work it was shown that photoautotrophical growth is slower in D61N and D61A than in WT and that D61A cells are further impaired in the absence of Ca^{2+}. Oxygen evolution under continuous illumination is decreased in D61N, D61A, and D61E to 17 ± 2%, 19 ± 6%, and 61 ± 5% of WT, respectively. On the basis of fluorescence measurements, it was concluded that all reaction centers in the cells of all three mutants contain photooxidizable Mn, that at least one S-state transition is slowed drastically in D61N and D61A cells, that the reduction of P_{680}^+ in hydroxylamine-treated cells is unchanged, and that the midpoint potential of S_2/S_1 is slightly increased in all three mutants, especially in D61N.

This work investigated these mutants from D1−D61 both in cells and in oxygen-evolving core particles. To gain detailed insight into the effect of mutations on the various partial reactions, the rates of electron transfer from Y_Z to P_{680}^+ and from the OEC to Y_Z^{ox} were measured at ns-time resolution and at μs- to ms-time resolution, respectively, in PSII core particles isolated from WT and D61N cells.

2. MATERIALS AND METHODS

Growth of Synechocystis sp. PCC 6803 Cells and Preparation of PSII Core Particles. Cells of the unmodified WT and the mutants of *Synechocystis* were cultivated as described by ref *20* but in an atmosphere enriched with 4% of CO_2

† Financial support of the Deutsche Forschungsgemeinschaft (Grant SFB 171/A2) and the Fonds der Chemischen Industrie to the laboratory of W.J. and of the NIH (Grant GM43496) to the laboratory of R.J.D. is gratefully acknowledged.

* Corresponding author. Tel.: +49-541-9692872. Fax: +49-541-9691221. E-mail: JUNGE@UOS.DE.

‡ Universität Osnabrück.

§ University of California.

[1] Abbreviations: chl, chlorophyll; DCBQ, 2,5-dichloro-*p*-benzoquinone; DM, *N*-dodecyl-β-D-maltoside; fwhm, full width at half-maximum; Hepes, *N*-(2-hydroxyethyl)piperazin-*N*′-2-ethanesulfonic acid; Mes, 2-*N*-morpholinoethanesulfonic acid; Mn, manganese; OEC, oxygen-evolving complex = Mn_4X-entity; OGP, *N*-octyl-β-D-glucopyranoside; PSI, photosystem I.; PSII, photosystem II.; Q_A, primary quinone acceptor; S_i, *i*th oxidized state of the OEC.; UV, ultraviolet; X, redox cofactor of the donor side; Y_Z, D1-tyrosine-161; WT, wild-type.

S0006-2960(98)01164-7 CCC: $15.00
Published on Web 09/23/1998

under illumination from fluorescent light (cool-white) at 0.8−1.4 mW cm^{-2}. The medium was supplemented with 5 mM glucose only for the growth of the mutants. Oxygen-evolving PSII core particles from cells (8−10 L, OD_{740} = 0.9−1.4) from *Synechocystis* were prepared by a procedure similar to that described in ref *21*. Cells were broken with glass beads with a diameter of 500 μm instead of 100 μm. For the mutant D61N the ratio of *n*-dodecyl-β-D-maltoside (DM):*n*-octyl-β-D-glucopyranoside (OGP):chlorophyll (chl) of 1.25:5:1 (w/w) resulted in a very low yield of PSII, which was improved by a ratio of 1.5:6:1 (w/w).

Oxygen evolution of PSII core particles with continuous saturating illumination was measured with a Clark-type electrode at 21 °C. Frozen and thawed PSII particles (2 μM chl) were suspended in 1 M sucrose, 50 mM Mes pH 6.5, 25 mM $CaCl_2$, 10 mM NaCl. 2,5-Dichloro-*p*-benzoquinone (DCBQ, 1 mM) was used as electron acceptor (with 2,6-DCBQ the rates of oxygen evolution were similar). Typical rates were 600−1400 μmol of O_2/(mg of chl·h) for WT and 120−300 μmol of O_2/(mg of chl·h) for D61N. These rates were correlated in reciprocal fashion with the ratio of 140−300 chl/PSII measured with repetitive excitation at 827 nm (with an extinction coefficient of 6000−7000 M^{-1} cm^{-1} (*22*, *23*)) at a time resolution of 4 ns per address (see below) with eight preparations.

Flash-induced release of oxygen was measured polarographically with a bare platinum electrode with cells (40 μL, 25 μM chl in 20 mM Hepes pH 7.2, 10 mM NaCl, 1 mM $CaCl_2$) that had been dark-adapted for 10 min. To increase its time resolution, the cells were packed upon the metal by centrifugation. The cathode (Pt) was polarized with −800 mV vs the anode (Ag/AgCl). The extent of oxygen evolution as function of flash number was measured with a series of 15 flashes from a Xenon-flash lamp (fwhm 10 μs, Schott GG420, 300 ms between flashes). Polarographic transients were digitized and recorded with a time resolution of 500 μs/address. The rate of oxygen release after the third flash was recorded at a higher time resolution, namely 100 μs/address (Xenon-flash lamp, Schott RG610, 1 s between flashes). A total of 5−10 recordings were averaged. Pattern of oxygen release were fitted with three Kok parameters (percentage of misses (α), double hits (β), and the distribution of S-states after dark-adaptation (% S_1) according to ref *24*). The measurements (with a maximum duration of 5 min) were done at room temperature (ca. 20 °C).

For flash-spectrophotometric measurements (*25*) PSII core particles were suspended in 20 mM Mes pH 6.35, 20 mM $CaCl_2$, 5 mM $MgCl_2$, 0.06% DM (w/v), in the presence or absence of 25% glycerol (v/v). Ferricyanide and/or DCBQ were used as electron acceptors as indicated. The measurements (with a maximum duration of 15 min) were done at room temperature (ca. 20 °C). Electron transfer from OEC to Y_Z^{ox} was recorded at 360 nm with five saturating flashes (100 ms between flashes) with repetitive (−glycerol, 25 s dark) or long-time (+glycerol, 10 min dark) dark-adapted samples (10 μM chl) (*26*) with a Xenon flash lamp (fwhm 10 μs, RG610) and an optical path length of 1 cm. The reduction of P_{680}^+ was measured as described in ref *23* with PSII core particles (30−40 μM) at 827 nm under repetitive saturating excitation (Nd:YAG laser, fwhm 6 ns, 532 nm, 300 ms between flashes) in the absence of glycerol (optical path length 5 cm) with DCBQ (200 μM) and ferricyanide (1 mM) as electron acceptors (time resolution 4 ns/address). Photometric transients were digitized on a Nicolet Pro30 or a Tectronics DSA602 recorder, and up to 200 signals were averaged.

The fits and the standard errors of the data sets were obtained by standard routines of the program Origin (Microcal).

3. RESULTS

3.1. WT and D61N retained oxygen evolution capacity after preparation of PSII core particles. Under saturating continuous light PSII core particles from wild-type showed rates of oxygen evolution of 600−1400 μmol of O_2/(mg of chl·h). The variation of this rate was reciprocal to the variable content of chlorophyll per PSII, which in turn was attributable to variable contamination with PSI as described in ref *21*. Core particles from the mutant D61N released oxygen at a rate of 120−300 μmol of O_2/(mg of chl·h). When normalized on the basis of chlorophyll per PSII, the mutant D61N core particles released oxygen at 20 ± 7% of WT. The same reduction, namely 18 ± 4%, was observed between whole cells of D61N and WT after normalization for the slightly lower PSII content of D61N cells (*19*).

It has been suggested that Asp61 may participate in binding of the cofactor Ca^{2+} (*19*). We checked whether the reduced rate of oxygen evolution in D61N was sensitive to variations of the concentration of Ca^{2+}. When the concentration of $CaCl_2$ was increased to 50, 100, or 200 mM (final concentrations), the rates of oxygen evolution decreased in both WT and D61N PSII core particles both from WT and D61N (to 85, 70, and 50%, compared to 25 mM $CaCl_2$, respectively). The inhibitory effect of moderate concentrations of Ca^{2+} on cyanobacterial PSII particles has been observed previously (*27*, *28*). Because high concentrations of Ca^{2+} (1 M) remove the extrinsic proteins from PSII (*29*), we speculate that the decreased rates of oxygen evolution in the presence of 50−200 mM $CaCl_2$ may be caused by partial detachment of the extrinsic 33 kDa polypeptide. A similar suggestion was made previously (*27*). Because the inhibitory effect of Ca^{2+} was the same in WT and D61N PSII core particles, we could obtain no information about a role for Ca^{2+} at Asp61. Because the concentrations of Ca^{2+} (up to 200 mM) were much greater than the two sets of dissociation constants (*K*) for Ca^{2+} as reported for various PSII preparations [namely $K_1 < 1$ μM and $K_2 < 10$ mM (see ref *30* and references therein)], our experiments were not designed to discover small alteration of the dissociation constant in the mutant.

3.2. Flash-induced release of oxygen was much slower with cells of D61N than of WT. Figure 1 shows polarographic currents of a bare Pt electrode in response to the O_2 production induced by the third flash given to dark-adapted cells, which were pelleted to its surface. The transient peak, lasting for less than 400 μs, was due to an intrinsic photoelectric effect of the Ag/AgCl anode (for a review see ref *31*). The following slower rise was attributable to the reduction of flash-induced oxygen by the electrode. We assumed that this transient with an effective half-rise time of 2.7 ± 0.5 ms for WT (Figure 1, top, left) resulted from two consecutive first-order reactions, (1) the production of

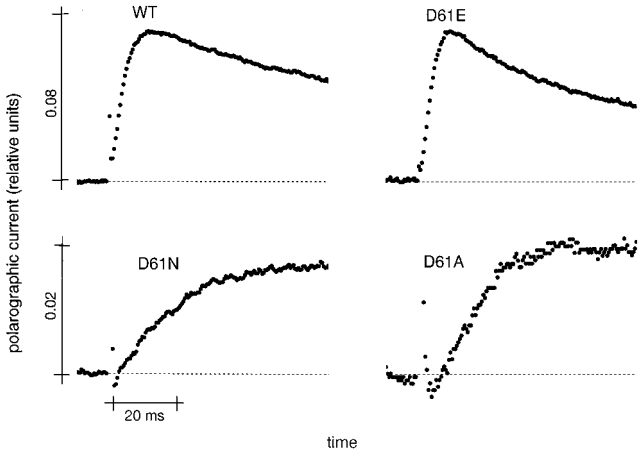

FIGURE 1: Flash-induced release of oxygen of WT (left, top), D61E (right, top), D61N (left, bottom), and D61A (right, bottom) on the third flash given to dark-adapted cells (40 μL with 25 μM chl) that were centrifuged on a bare platin electrode (time resolution 100 μs/address, every fifth point shown, 5 measurements averaged). The transients revealed effective half-rise times of 2.7 $\pm$ 0.5 ms for WT and D61E and longer half-rise times for D61N (15 $\pm$ 1 ms) and D61A (12 $\pm$ 1 ms) (Table 1).

Table 1: Half-Rise Times of Oxygen Release on $S_3 \Rightarrow S_0$[a]

	effective $t_{1/2}$ (ms)	intrinsic $t_{1/2}$ (ms)
WT	2.7 $\pm$ 0.5	1.2 $\pm$ 0.5
D61E	2.7 $\pm$ 0.5	1.2 $\pm$ 0.5
D61A	12 $\pm$ 1	10.5 $\pm$ 1
D61N	15 $\pm$ 1	13.5 $\pm$ 1

[a] Half-rise times of oxygen release were measured with cells of WT, D61E, D61A, and D61N (Figure 1). The effective half-rise time was attributed to two consecutive reaction, the release of oxygen (intrinsic half-rise time) and diffusion of produced oxygen to the electrode ($t_{1/2} \approx$ 1.5 ms; see section 3.2).

oxygen (rate constant k_1) and (2) the diffusion of the oxygen to the electrode (rate constant k_2). Because the oxygen-evolving transition, $S_3 \Rightarrow S_0$, in WT proceeds with an intrinsic half-rise time of $t_{1/2}$ = 1.2−1.5 ms (as judged from measurements in the UV (*32*−*34*) and as shown previously for wild-type core particles; see Table 2) we attribute the difference between 2.7 ms and 1.2−1.5 ms to the second reaction, the diffusion of oxygen from the pelleted layer of cells to the electrode. The expected transient based on standard chemical kinetics was as follows (*35*):

$$\frac{y(t)}{y(\infty)} = 1 + \frac{1}{k_2 - k_1}[k_1 e^{-k_2 t} - k_2 e^{-k_1 t}]$$

The expected lag phase was not resolved because it was submerged under the flash burst artifact. Therefore we used the gross notion that the effective half-rise time was simply the sum of the intrinsic and diffusive ones. Because the cell diameter of all mutants was about 1.5-times larger than the one of the WT (data not shown), their packing on the electrode might differ. Whether this bears on the more rapid decay of the polarographic transient in D61E as compared with WT (see Figure 1) remains to be established. For the following interpretation of our data it was more important that the *rise time* of the transients in D61E (larger cells) and WT (standard cell size) was the same within error limits. Accordingly we took the diffusive rise time of WT as the upper limit for the diffusive time.

Assuming that the same diffusive half-rise time, 1.5 ms, also holds for cells of the mutant D61N, we determined an intrinsic half-rise time of oxygen release of about 13.5 $\pm$ 1 ms from the effective half-rise time of 15 $\pm$ 1 ms of the transient in Figure 1 (left, bottom). A simulation of the consecutive first-order reactions using the above parameters produced a viable fit; the predicted lag-phase, however, was hidden by the photoelectric artifact. In the mutant D61E the polarographic transient (Figure 1, right, top) rose with a similar half time as observed with cells of WT. D61A exhibited a much slower rise with an effective half-rise time of 12 $\pm$ 1 ms (Figure 1, right, bottom) (Table 1); it also exhibited a much slower decay. This parallel behavior of the rise and the decay was predicted by ref *36* on the basis of a theory of reaction−diffusion under the assumption of the same packing behavior on the surface of the polarographic electrode.

At a first sight it was puzzling that the maximum extent of the polarographic transient per flash in D61E was the same as the one in WT although the total oxygen yield under continuous illumination was only 61% (or specifically 75% when weighted with apparent PSII content of 80%) in the former (*19*). It is an interesting question whether the difference was attributable to the fact that the latter work was based on modified WT* cells grown on glucose whereas we used unmodified WT cells grown without glucose.

Table 2: Distribution of S-States after Dark Adaptation and Factor of Misses (α) and Double Hits (β) (So-Called Kok Parameters) and Half-Rise Times of Electron Transfer OEC $\rightarrow Y_Z^{ox}$ and $Y_Z \rightarrow P_{680}^+$ upon Flash Excitation of Cells and Core Particles of WT and D61N[a]

	WT	D61N
$S_0/S_1/S_2/S_3$ (in %) (cells, −G)	27/73/0/0 ($\pm$5)	21/79/0/0 ($\pm$5)
misses = α (in %) (cells, −G)	17 $\pm$ 2	26 $\pm$ 2
double hits = β (in %) (cells, −G)	4 $\pm$ 1	10 $\pm$ 1
$S_1 \Rightarrow S_2$ (cores, −G)	100 $\pm$ 30 μs	240 $\pm$ 50 μs
$S_2 \Rightarrow S_3$ (cores, −G)	220 $\pm$ 30 μs	520 $\pm$ 50 μs
$S_3 \Rightarrow S_0$ (cores, +G)	1.5 $\pm$ 0.1 ms[b]	n.d.
$S_3 \Rightarrow S_0$ (cores, −G)	4.5 $\pm$ 0.4 ms[b]	n.d.
reduction of P_{680}^+ (cores, −G)	28 $\pm$ 5 ns (53%)	28 $\pm$ 5 ns (45%)
	320 $\pm$ 40 ns (16%)	240 $\pm$ 40 ns (21%)
	>3 μs (31%)[c]	>3 μs (34%)[c]

[a] The fits of flash-induced release of oxygen (Figure 2) revealed similar S-state distribution but significantly increased misses and seemingly increased double hits (see section 3.2) for D61N. Half-rise times of electron transfer from OEC to Y_Z^{ox} on the first flash (mainly $S_1 \Rightarrow S_2$) and second flash (mainly $S_2 \Rightarrow S_3$) were increased in PSII core particles from D61N compared to WT (Figure 3; in the absence of glycerol). Half-rise times of the oxygen-producing transition $S_3 \Rightarrow S_0$ was measured in PSII core particles from WT in the presence of glycerol (+G) and its absence (−G). Electron transfer from Y_Z to P_{680}^+ (repetitive excitation) was not altered in PSII core particles from D61N (Figure 4; in the absence of glycerol). [b] Data from ref *34*. [c] Percentage of slow phases ($t_{1/2}$ > 3 μs) = upper limit for inactive PSII (see section 4.1.).

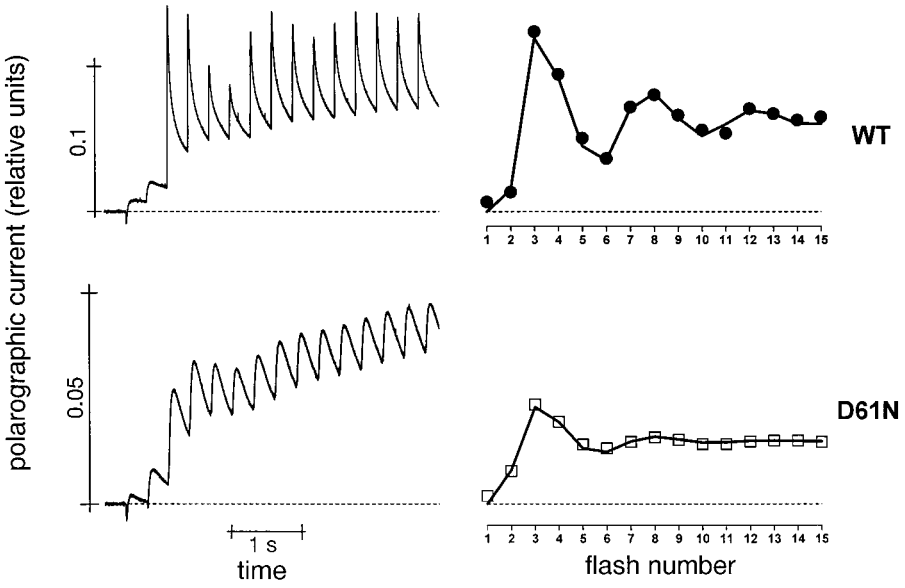

FIGURE 2: Flash-dependent pattern of oxygen release of cells of WT (top) and D61N (bottom) with the original traces (left) and the fits (solid lines, right) of the amount of oxygen produced by the WT (closed circles, right) or D61N (open squares, right). Fifteen flashes with a distance of 300 ms were given. The fits revealed a similar equilibrium of the states S_0/S_1 after dark-adaptation of 27/73 ± 5 (WT) or 21/79 ± 5 (D61N) but an increased degree of misses ($\alpha = 26 \pm 2\%$ vs $17 \pm 2\%$) and double hits ($\beta = 10 \pm 1\%$ vs $4 \pm 1\%$) for D61N compared to WT (Table 2). Time resolution was 500 μs/address; 10 measurements were averaged.

Patterns of flash-induced oxygen release with cells of WT and D61N (Figure 2, left traces, top and bottom) were compared. The flash-dependent oxygen yield was taken from the maximal amplitude, not from the area beneath the curve. Flash-dependent oxygen yield (in relative units) of WT (closed circles) and D61N (open squares) (Figure 2, right) were fitted (Figure 2, right, solid lines). The equilibrium of the S-states after dark-adaptation was not greatly altered for WT and D61N. The distributions of $S_0/S_1/S_2/S_3$ were 27/73/0/0 and 21/79/0/0 (Table 2), respectively, being similar to that of thylakoids from higher plants (*37*, *38*). The most drastic difference was the stronger damping in D61N (Figure 2, bottom) than for WT (Figure 2, top). It was mainly attributable to a higher degree of misses ($\alpha = 26 \pm 2\%$ for D61N vs $17 \pm 2\%$ for WT, Table 2). We believe that the calculated increase of double hits for D61N ($\beta = 10 \pm 1\%$ vs $4 \pm 1\%$ in WT) may be an artifact caused by using the same miss factor, α, for each S-state transition. Because oxygen release in D61N was about 10-fold slower than in WT, it is more likely that competition for Y_Z^{ox} reduction by reductants other than the OEC increased the miss factor predominantly on $S_3 \Rightarrow S_0$ (see section 4.2).

The decay of the transient of D61N was slower than of WT (Figure 2, left traces). This observation coincided with calculations of ref *36*, in which a decreased intrinsic rate of oxygen release is accompanied with a decreased rate of the decay of the polarographic signal. The slow decay did not cause the higher factor of misses in D61N in the time span of 300 ms between flashes because measurement with a spacing of 600 ms between the flashes gave a similar result as with 300 ms, namely $S_0/S_1/S_2/S_3 = 22/78/0/0$ (±5), $\alpha = 27 \pm 2\%$, and $\beta = 10 \pm 1\%$ (data not shown).

3.3. Increased Half-Rise Times of $S_1 \Rightarrow S_2$ and $S_2 \Rightarrow S_3$ in PSII Core Particles from D61N Compared to WT. Flash-induced absorption transients at 360 nm (Figure 3, closed circles) on the first two flashes given to repetitively dark-adapted (see Material and Methods) PSII core particles of WT (top traces) and D61N (bottom traces) were fitted (solid lines) with two exponentials. The rapid processes ($t_{1/2} < 20$ μs, indicated by the dashed line in Figure 3), namely the reduction of the primary quinone acceptor (Q_A) (on first and second flash) and oxidation of photosystem I (PSI) (on first flash), were not resolved (time resolution 20 μs/address). The extent of this fast component was higher on the first flash of D61N than of WT, and it was generally higher on the first flash than on the second one. This was due to the variations of the content of PSI and inactive PSII, which were both oxidized only on the first flash. The slow phase, indicating the oxidation of the OEC, was decreased on the first flash (Figure 3, left) from $t_{1/2} = 100 \pm 30$ μs (WT, $-\Delta I/I = 2.8 \times 10^{-4}$) to 240 ± 50 μs (D61N, $-\Delta I/I = 2 \times 10^{-4}$) and on the second flash (Figure 3, right) from 220 ± 30 μs (WT, $-\Delta I/I = 2.3 \times 10^{-4}$) to 520 ± 50 μs (D61N, $-\Delta I/I = 1.3 \times 10^{-4}$) (Table 2). Due to the accumulation of S_1 in the dark, both in WT and D61N (Figure 2, Table 2), these slow phases primarily resulted from $S_1 \Rightarrow S_2$ on the first flash and from $S_2 \Rightarrow S_3$ on the second one. The half-rise times of WT of *Synechocystis* for $S_1 \Rightarrow S_2$ and $S_2 \Rightarrow S_3$ (100 ± 30 μs and 220 ± 30 μs) were compatible with the one reported for higher plants ($t_{1/2} = 90-110$ μs for $S_1 \Rightarrow S_2$ and 130−380 μs for $S_2 \Rightarrow S_3$ (*32*, *33*, *39*−*41*)).

3.4. Reduction of P_{680}^+ was similar in PSII core particles from WT and D61N. The reduction of P_{680}^+ was analyzed by absorption transients at 827 nm (Figure 4) with repetitively excited PSII core particles from WT (left) and D61N (right). The smaller extent of the absorption transients in D61N ($-\Delta I/I = 4.5 \times 10^{-3}$) compared to WT ($-\Delta I/I = 9.5 \times 10^{-3}$) was due to a higher ratio of PSI/PSII in core preparations from D61N. In the presence of ferricyanide (≥ 50 μM) more than 95% of P_{700} was oxidized before the flash under repetitive excitation (checked at 700 nm, data not shown). The decay of the transients from WT were fitted with three exponentials with half-rise times of 28 ± 5 ns (53%), 320 ± 40 ns (16%), and > 3 μs (31%). The fit for

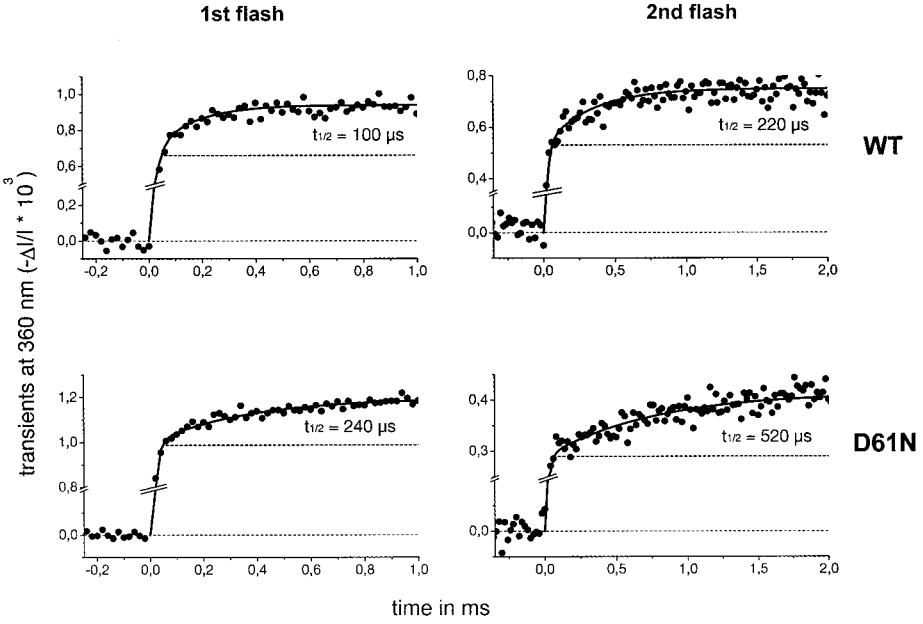

FIGURE 3: Increased half-rise times of electron transfer from OEC to Y_Z^{ox} observed at 360 nm on the first flash (left traces) and the second one (right traces) in repetitively dark-adapted PSII core particles (−glycerol) from D61N (bottom) compared to WT (top). The slow phases (indicated by the dashed line) on the first and second flash, representing mainly the transitions $S_1 \Rightarrow S_2$ and $S_2 \Rightarrow S_3$, were fitted with $t_{1/2} = 100 \pm 30$ μs and 220 ± 30 μs for WT and 240 ± 50 μs and 520 ± 50 μs for D61N (Table 2). DCBQ (200 μM) was used as electron acceptor; the time resolution was 20 μs/address. Transients were an average of 100 (WT) or 200 (D61N) measurements.

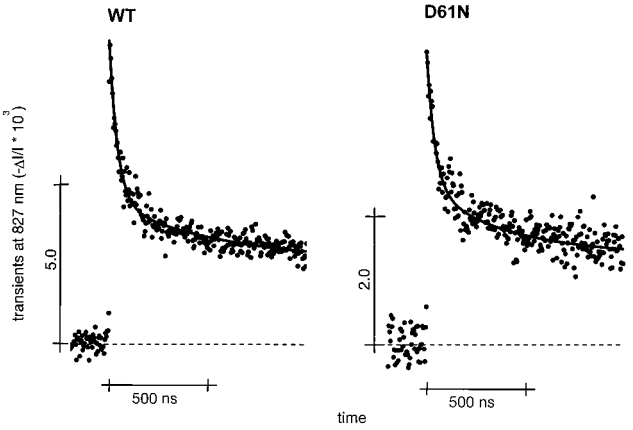

FIGURE 4: Similar half-rise times of reduction of P_{680}^+ were measured at 827 nm in PSII core particles from D61N and WT. PSII core particles from WT (30 μM chl, left trace) and D61N (40 μM chl, right trace) were repetitively excited (300 ms between flashes) in the absence of glycerol with a time resolution of 4 ns/address. The data (closed circles) were fitted (solid lines) with half times of 28 ± 5 ns (53%), 320 ± 40 ns (16%), and >3 μs (31%) for WT and 28 ± 5 ns (45%), 240 ± 40 ns (21%), and >3 μs (34%) for D61N (Table 2). DCBQ (200 μM) and ferricyanide (1 mM) served as electron acceptors; 150 (WT) or 200 (D61N) measurements were averaged.

D61N gave 28 ± 5 ns (45%), 240 ± 40 ns (21%), and > 3 μs (34%) (Table 2). With PSII core particles from WT that were prepared according to another procedure (*28*), we obtained a fit with 33 ± 4 ns (55%), 320 ± 40 ns (16%), and >3 μs (29%) (data not shown). PSII core particles from pea (*26*, *42*) showed no significant difference in the ns-components with 37 ± 5 ns (57%) and 320 ± 30 ns (22%), but the amount of the slow components (>3 μs) was somewhat less (21%) (data not shown).

4. DISCUSSION

4.1. Oxygen-Evolving Activity of PSII Core Particles from WT and D61N from Synechocystis. Flash-photometric experiments are specific and time-resolving for electron- and proton-transfer reactions involving the OEC, Y_Z, and P_{680}. However, for reasons of signal-to-noise or signal-to-artifact they are difficult to perform with whole cells and thus necessitate core preparations. The latter, on the other hand, may suffer from additional modifications during the preparation procedure, in particular when mutants serve as starting material. We checked the activity of core preparations of WT and D61N by measuring oxygen evolution and reduction of P_{680}^+. The relative rate of oxygen evolution under continuous illumination of D61N compared to WT was almost the same in PSII core particles (20 ± 7% of WT; see section 3.1) and in cells (18 ± 4% of WT (*19*)). The proportion of inactive PSII (upper limit) has been assessed by the relative extent of the slow reduction of P_{680}^+ ($t_{1/2} > 3$ μs) as known from the literature (*43*−*45*). It was only slightly increased in PSII core particles from D61N compared to WT (34 vs 31%, Figure 4 and Table 2). This small difference could be due to a higher equilibrium ratio of $P_{680}^+S_i/P_{680}S_{i+1}$ in D61N as it was reported in ref *19*, probably caused by an increased midpoint potential of approximately 30 mV of the OEC (see section 4.2). The percentage of the slow component (approximately 30%) did not depend on the type of preparation because PSII core particles from WT prepared according to another procedure (*28*) revealed 29% of the slow components. The microsecond components of P_{680}^+ reduction may significantly overestimate the proportion of inactive PSII in the preparations. One microsecond component ($t_{1/2} = 30$ μs) oscillates with S-state (*44*) and has been suggested to arise from an S-state-dependent equilibrium between $Y_ZP_{680}^+$ and $Y_Z^{ox}P_{680}$ (see ref *46*). On the basis of O_2 flash-yield measurements, Mn quantitation, and the absence of photoaccumulation of Y_Z^{ox} at room temperature, Tang and Diner (*28*) concluded that their *Synechocystis* PSII particles contained essentially no inactive PSII. The lower amount of slow P_{680}^+ reduction in PSII

core particles from pea (*26*, *42*) of 21% (see section 3.4) may indicate a higher stability of PSII from pea, a greater damage to PSII from *Synechocystis* because of harsher preparation techniques, or a diffence in the S-state dependent equilibrium between Y_Z^{ox} and P_{680}^+ in *Synechocystis* and pea.

4.2. The S-state transitions were slowed in D1-D61N. Fluorescence measurements with D61N had shown that at least one S-state transition was drastically slowed (*19*); however, its nature has remained ill-defined.

In core particles from WT we found that the half-rise times of transitions $S_1 \rightarrow S_2$ (100 ± 30 μs) and $S_2 \rightarrow S_3$ (220 ± 30 μs) (Figure 3, Table 2) were similar to the half-rise times measured with material from higher plants (90−110 μs for $S_1 \rightarrow S_2$ and 180−380 μs for $S_2 \rightarrow S_3$ (*23*, *32*, *33*, *39*, *41*)). However, in the mutant D61N these half-rise times were 240 μs/520 μs (Figure 3, Table 2), i.e., increased by factors of approximately 2.4. From fluorescence decay kinetics in D61N it was concluded that the midpoint potential of S_2/S_1 is slightly increased (*19*). In terms of the theory of nonadiabatic electron transfer (*47*) and assuming that the distances and reorganization energies are unchanged, the slowing of $S_1 \rightarrow S_2 \rightarrow S_3$ by a factor of 2.4 (Figure 3, Table 2) implies an increase of the respective midpoint potentials of S_2/S_1 and S_3/S_2 by approximately 30 mV.

Oxygen release in D61N occurred with a half-rise time of $t_{1/2} \approx 13.5$ ms, i.e., about 10 times longer than in WT ($t_{1/2} = 1.2-1.5$ ms) (Figure 1, Table 1). This is the slowest rate of oxygen release ever reported for cells or PSII preparations. For technical reasons we were unable to determine the half-rise time of the reduction of Y_Z^{ox} in $S_3 \rightarrow S_0$ in D61N at 360 nm, mainly because of the high frequency of misses. In other systems where it was possible to determine in parallel the rates of oxygen release and of Y_Z^{ox} reduction, they were coincident, e.g. in thylakoids, BBY-membranes ($t_{1/2} = 1-1.5$ ms), and core particles ($t_{1/2} = 4.5$) from higher plants and cells of the ΔpsbO-mutant of *Synechocystis* ($t_{1/2} = 6-10$ ms) (*33*, *48*−*51*). The average factor of misses in the pattern of oxygen release in the D61N mutant was increased by 9% (Figure 2, Table 2). This factor was calculated with the assumption that it is independent of S-state. However, if the reduction of Y_Z^{ox} during the $S_3 \rightarrow S_0$ transition is slowed as drastically as O_2 release, then the increase in misses may occur almost entirely during the $S_3 \rightarrow S_0$ transition and be caused by the reduction of the long-lived Y_Z^{ox} by a competitive reductant (R) either directly or indirectly via P_{680}^+. If Y_Z^{ox} is reduced directly by R, then a parallel reaction scheme would apply:

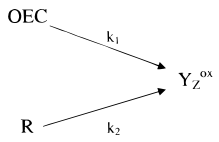

Here Y_Z^{ox} is reduced by the OEC with a rate constant k_1, to yield oxygen, or by R with rate constant k_2. The effective rates of both Y_Z^{ox} reduction and oxygen release would be $k = k_1 + k_2$. This implies that the rate constant for OEC oxidation during $S_3 \rightarrow S_0$, k_1, is smaller than the effective rate of oxygen release, so that the half-time for OEC oxidation during $S_3 \rightarrow S_0$ in D61N would be longer than the observed 13.5 ms half-rise time of oxygen release.

The drastic slowing of oxygen release in D61N could be caused by the summation of two effects: (1) an increase of the midpoint potential of the OEC of approximately 30 mV (see above, factor ≈ 2−3) as in the other transitions plus (2) the sensitivity of O−O bond formation to nuclear and electronic reorganizations of the OEC. The latter explanation was presented in refs *34* and *40* for the slowing of $S_3 \rightarrow S_0$ (by a factor of 3−4) in PSII core particles from higher plants (*26*, *39*) and in PSII core particles from WT of *Synechocystis* in the absence of glycerol (Table 2 and (*34*)).

Possible explanations for an increased midpoint potential of the OEC in some or all S-states are, e.g., (1) a direct electrostatic effect due to the replacement of the negatively charged amino acid at position 61 with a neutral one or (2) an indirect effect through the altered binding of Ca^{2+} (*19*). Both hypotheses are supported by the drastic effect on the rate of oxygen release under continuous illumination (*19*) and under flashing light (see section 3.2 and Table 1). This was observed when aspartate was mutated to asparagine or alanine, whereas the mutation to glutamate showed no or little effect.

An increased half-rise time of oxygen release ($t_{1/2} = 6-12$ ms) has been reported for a mutant lacking the extrinsic 33 kDa protein (ΔpsbO (*51*−*53*)) and another single site mutant of the D1-protein (D1-R334V (*54*)). The slower release of oxygen was likewise accompanied by a higher miss factor in the pattern of oxygen release in D61N (26 vs 17%, this work, Figure 2) and in ΔpsbO (22 vs 15% (*52*)). An increase of the average half-rise time of transitions $S_0 \rightarrow S_1 \rightarrow S_2 \rightarrow S_3$ was described for ΔpsbO cells (400 μs) compared to WT (140 μs) (*51*). These similarities between D1−D61N (this work) and ΔpsbO mutants (see above) are probably not attributable to the loss of the extrinsic 33 kDa protein in D61N, because (1) raising the concentration of Ca^{2+}, which probably partially removed the extrinsic proteins (*27*), diminished the oxygen-evolving activity in both WT and D61N PSII core particles (see section 3.1). (2) Also, the oxygen-evolving activitiy of D61N cells exhibits the same stability in the darkness as WT (*19*), whereas ΔpsbO cells lose activity rapidly in darkness (*20*, *53*, *55*). (3) Oxygen-evolving PSII core particles could be isolated from D61N cells using essentially the same isolation procedure as used for WT. In contrast, the oxygen-evolving activity of ΔpsbO cells is lost during cell breakage unless the cells are broken in the presence of 0.5 M NaCl (*55*).

4.3. Mutation D61N influenced the OEC but not Y_Z or P_{680}. The rate of electron transfer from OEC to Y_Z^{ox} was slowed during $S_1 \rightarrow S_2$, $S_2 \rightarrow S_3$, and possibly during $S_3 \rightarrow S_0$ in D61N compared to WT (Figures 1 and 3, Tables 1 and 3), whereas the rate of P_{680}^+ reduction by Y_Z was similar in D61N and WT (Figure 4, Table 2). These results probably imply that neither the ligation sphere nor the dielectric environment of Y_Z and P_{680} was changed; therefore, the mutation D61N selectively affected the OEC (Mn_4X-entity).

5. CONCLUSIONS

A point mutation D1−D61N, located between helices A and B of the D1 protein at the donor side of PSII, drastically slowed oxygen release by a factor of 9−10. The transitions $S_1 \rightarrow S_2$ and $S_2 \rightarrow S_3$ were also slowed by a factor of 2−3. On the other hand, the reduction of P_{680}^+ by Y_Z was unaffected.

If the drastically slowed rate of oxygen release in D61N cells is caused by a drastically prolonged lifetime of Y_Z^{ox} ($t_{1/2} \approx 13.5$ ms) during the $S_3 \rightharpoonup S_0$ transition (without disturbance of Y_Z and P_{680}), then further characterization of D61N core particles could give a new approach to characterize the radical Y_Z^{ox} and its environment in *oxygen-evolving* PSII. Attempts to measure the rate of Y_Z^{ox} reduction during $S_3 \rightharpoonup S_0$ are underway.

NOTE ADDED IN PROOF

Simulations of the absorption transients with core particles of WT and D1−D61N at 360 nm (third flash) show that the reduction of the OEC in $S_3 \rightharpoonup S_0$ occurred with a similar half-time ($t_{1/2} \approx 13$ ms) as oxygen release and suggest that the reduction of Y_Z^{ox} in $S_3 \rightharpoonup S_0$ was slowed to a similar extent (see ref *56*).

ACKNOWLEDGMENT

We thank Hella Kenneweg for excellent technical assistance and R. Ahlbrink, Drs. O. Bögershausen, W. Drevenstedt, M. Haumann, and A. Mulkidjanian for helpful discussions.

REFERENCES

1. Debus, R. J. (1992) *Biochim. Biophys. Acta 1102*, 269−352.
2. Yachandra, V. K., Sauer, K., and Klein, M. P. (1996) *Chem. Rev. 96*, 2927−2950.
3. Britt, R. D. (1996) in *Oxygenic photosynthesis: The light reactions* (Ort, D., and Yocum, C. F., Eds.) pp 137−164, Kluwer, Dordrecht, The Netherlands.
4. Renger, G. (1997) *Physiol. Plant. 100*, 828−841.
5. Rhee, K. H., Morris, E. P., Zheleva, D., Hankamer, B., Kuhlbrandt, W., and Barber, J. (1997) *Nature 389*, 522−526.
6. Svensson, B., Etchebest, C., Tuffery, P., van Kan, P., Smith, J., and Styring, S. (1996) *Biochemistry 35*, 14486−14502.
7. Xiong, J., Subramaniam, S., and Govindjee (1996) *Protein Sci. 5*, 2054−2073.
8. Michel, H., and Deisenhofer, J. (1988) *Biochemistry 27*, 1−7.
9. Berthomieu, C., and Boussac, A. (1995) *Biochemistry 34*, 1541−1548.
10. Durrant, J. R., Klug, D. R., Kwa, S. L. S., van Grondelle, R., Porter, G., and Dekker, J. P. (1995) *Proc. Natl. Acad. Sci. U.S.A. 92*, 4798−4802.
11. Mulkidjanian, A. Y., Cherepanov, D. A., Haumann, M., and Junge, W. (1996) *Biochemistry 35*, 3093−3107.
12. Konermann, L., Yruela, I., and Holzwarth, A. R. (1997) *Biochemistry 36*, 7498−7502.
13. Dau, H., Andrews, J. C., Roelofs, T. A., Latimer, M. J., Liang, W., Yachandra, V. K., Sauer, K., and Klein, M. P. (1995) *Biochemistry 34*, 5274−5287.
14. Kodera, Y., Hara, H., Astashkin, A. V., Kawamori, A., and Ono, T. (1995) *Biochim. Biophys. Acta 1232*, 43−51.
15. Smith, P. J., and Pace, R. J. (1996) *Biochim. Biophys. Acta 1275*, 213−220.
16. Tang, X. S., Randall, D. W., Force, D. A., Diner, B. A., and Britt, R. D. (1996) *J. Am. Chem. Soc. 118*, 7638−7639.
17. Zech, S. G., Kurreck, J., Eckert, H. J., Renger, G., Lubitz, W., and Bittl, R. (1997) *FEBS Lett. 414*, 454−456.
18. Trebst, A. (1986) *Z. Naturforsch. 41c*, 240−245.
19. Chu, H. A., Nguyen, A. P., and Debus, R. J. (1995) *Biochemistry 34*, 5839−5858.
20. Chu, H. A., Nguyen, A. P., and Debus, R. (1994) *Biochemistry 33*, 6137−6149.
21. Kirilovsky, D. L., Boussac, A., van Mieghem, F. J. E., Ducruet, J. M., Setif, P., Yu, J., Vermaas, W. F. J., and Rutherford, A. W. (1992) *Biochemistry 31*, 2099−2107.
22. Mathis, P., and Setif, P. (1981) *Isr. J. Chem. 21*, 316−320.
23. Haumann, M., Drevenstedt, W., Hundelt, M., and Junge, W. (1996) *Biochim. Biophys. Acta 1273*, 237−250.
24. Forbush, B., Kok, B., and McGloin, M. P. (1971) *Photochem. Photobiol. 14*, 307−321.
25. Junge, W. (1976) in *Chemistry and Biochemistry of Plant Pigments* (Goodwin, T. W., Ed.) pp 233−333, Academic Press, London, New York, San Francisco.
26. Bögershausen, O., and Junge, W. (1995) *Biochim. Biophys. Acta 1230*, 177−185.
27. Pauly, S., Schlodder, E., and Witt, H. T. (1992) *Biochim. Biophys. Acta 1099*, 203−210.
28. Tang, X. S., and Diner, B. A. (1994) *Biochemistry 33*, 4594−4603.
29. Ono, T., and Inoue, Y. (1983) *FEBS Lett. 164*, 255−260.
30. Grove, G. N., and Brudvig, G. W. (1998) *Biochemistry 37*, 1532−1539.
31. van Gorkom, H. J., and Gast, P. (1996) in *Biophysical techniques in photosynthesis* (Amesz, J., and Hoff, A. J., Eds.) pp 391−405, Kluwer Academic Publishers, Dordrecht, The Netherlands.
32. Dekker, J. P., Plijter, J. J., Ouwenand, L., and van Gorkom, H. J. (1984) *Biochim. Biophys. Acta 767*, 176−179.
33. Renger, G. and Weiss, W. (1986) *Biochim. Biophys. Acta 850*, 184−196.
34. Haumann, M., Hundelt, M., Jahns, P., Chroni, S., Bögershausen, O., Ghanotakis, D., and Junge, W. (1997) *FEBS Lett. 410*, 243−248.
35. Connors, K. A. (1990) in *Chemical kinetics*, VCH, New York.
36. Lavorel, J. (1992) *Biochim. Biophys. Acta 1101*, 33−40.
37. Messinger, J., and Renger, G. (1994) *Biochemistry 33*, 10896−10905.
38. Haumann, M., and Junge, W. (1994) *Biochemistry 33*, 864−872.
39. van Leeuwen, P. J., Heimann, C., Gast, P., Dekker, J. P., and van Gorkom, H. J. (1993) *Photosynth. Res. 38*, 169−176.
40. Haumann, M., Bögershausen, O., Cherepanov, D. A., Ahlbrink, R., and Junge, W. (1997) *Photosynth. Res. 51*, 193−208.
41. Razeghifard, M. R., and Pace, R. J. (1997) *Biochim. Biophys. Acta 1322*, 141−150.
42. van Leeuwen, P. J., Nieveen, M. C., van de Meent, E. J., Dekker, J. P., and van Gorkom, H. J. (1991) *Photosynth. Res. 28*, 149−153.
43. Conjeaud, H., and Mathis, P. (1980) *Biochim. Biophys. Acta 590*, 353−359.
44. Schlodder, E., Brettel, K., and Witt, H. T. (1985) *Biochim. Biophys. Acta 808*, 123−131.
45. Rappaport, F., Porter, G., Barber, J., Klug, D. R., and Lavergne, J. (1995) in *Photosynthesis: from light to biosphere* (Mathis, P., Ed.) pp 345−348, Kluwer, Dordrecht, The Netherlands.
46. Schilstra, M. J., Rappaport, F., Nugent, J. H. A., Barnett, C. J., and Klug, D. R. (1998) *Biochemistry 37*, 3974−3981.
47. Marcus, R. A., and Sutin, N. (1985) *Biochim. Biophys. Acta 811*, 265−322.
48. Babcock, G. T., Blankenship, R. E., and Sauer, K. (1976) *FEBS Lett. 61*, 286−289.
49. van Leeuwen, P. J., Heimann, C., and van Gorkom, H. J. (1993) *Photosynth. Res. 38*, 323−330.
50. Haumann, M. (1996) Thesis, Universität Osnabrück.
51. Razeghifard, M. R., Wydrzynski, T., Pace, R. J., and Burnap, R. L. (1997) *Biochemistry 36*, 14474−14478.
52. Burnap, R. L., Shen, J. R., Jursinic, P. A., Inoue, Y., and Sherman, L. A. (1992) *Biochemistry 31*, 7404−7410.
53. Engels, D. H., Lott, A., Schmid, G. H., and Pistorius, E. K. (1994) *Photosynth. Res. 42*, 227−244.
54. Burnap, R. L., Qian, M., Al-Khladi, S., and Pierce, C. (1995) in *Photosynthesis: from light to biosphere* (Mathis, P., Ed.) pp 443−446, Kluwer, Dordrecht, The Netherlands.
55. Burnap, R. L., Qian, M., Shen, J. R., Inoue, Y., and Sherman, L. A. (1994) *Biochemistry 33*, 13712−13718.
56. Hundelt, M., Hays, A.-M. A., Debus, R. J., and Junge, W. (1998) in *Photosynthesis: mechanisms and effects* (Garab, G., Ed.) Kluwer Academic Publishers, Dordrecht, The Netherlands (in press).

BI981164J